1995ApJ...443..499P

THE ASTROPHYSICAL JOURNAL, 443:499–513, 1995 April 20
© 1995. The American Astronomical Society. All rights reserved. Printed in U.S.A.

THE SPATIAL DISTRIBUTION OF BLUE COMPACT GALAXIES IN THE SECOND BYURAKAN SURVEY

SIMON A. PUSTIL'NIK, ANDREI V. UGRYUMOV, AND VALENTIN A. LIPOVETSKY
Special Astrophysical Observatory, Russian Academy of Sciences, Nizhnij Arkhyz, Karachai-Circessia 357147, Russia

TRINH X. THUAN
Astronomy Department, University of Virginia, Charlottesville, VA 22903, USA;
DAEC, Observatoire de Paris-Meudon; and Service d'Astrophysique, Centre d'Etudes de Saclay

AND

NATALIA G. GUSEVA
Main Astronomical Observatory, Ukranian Academy of Sciences, Goloseevo, Kiev, 252127 Ukraine
Received 1994 July 25; accepted 1994 October 28

ABSTRACT

We present the results of a study of the spatial distribution relative to bright normal galaxies of a new large sample of blue compact galaxies (BCGs) in the zone of the Second Byurakan Survey (SBS): $7^h40^m \leq \alpha \leq 17^h20^m$, $49° \leq \delta \leq 61.°2$, using as statistic the distance D_{NN} to the nearest neighboring bright galaxy. We found that the majority ($\sim$80%) of BCGs have $D_{NN} < 5\ h^{-1}$ Mpc and follow generally the large-scale structure delineated by bright galaxies, but that a minority ($\sim$20%) have $D_{NN} > 5\ h^{-1}$ Mpc and are found in voids. The large deficiency of BCGs with $D_{NN} \lesssim 2\ h^{-1}$ Mpc supports the hypothesis that the majority of dwarf galaxies originate as low-mass primordial density fluctuations, but not as debris resulting from tidal interactions between massive galaxies. The spatial distribution of BCGs is consistent with that found for low-surface-brightness dwarfs, supporting the idea that BCGs are LSB dwarfs undergoing intense bursts of star formation.

Subject headings: galaxies: clustering — galaxies: compact — galaxies: evolution — methods: statistical

1. INTRODUCTION

During the last decade, large systematic redshift surveys of bright galaxies (e.g., Huchra et al. 1983; de Lapparent, Geller, & Huchra 1986; da Costa et al. 1988; Fairall et al. 1990) have uncovered an extraordinary landscape where galaxies trace out large linear structures reaching dimensions of up to $\sim$50 Mpc such as the Great Wall (Ramella, Geller, & Huchra 1992), surrounding large voids of diameters $\sim$50 Mpc, completely empty of bright galaxies. At the same time, observational evidence together with theoretical arguments have been assembled which suggest that the universe may contain a considerable amount of dark matter whose mass can be as much as 100 times the mass of the luminous matter in stars and galaxies. (Trimble 1987; Ashman 1992, and references therein). The nature of this dark matter is still completely unknown, but propositions range from baryonic dark matter such as Jupiter-type objects or brown dwarfs, to cold dark matter (CDM) such as axions or WIMPs, to hot dark matter (HDM) such as massive neutrinos, to mixtures of these various types of dark matter.

If dark matter is the main constituent of the universe, it must greatly affect the processes of galaxy and large-scale structure formation. These processes differ in models with different types of dark matter, so that, in principle, these models can be tested. Until recently, CDM models were considered to be the most successful in reproducing known observational constraints such as the properties of galaxies of different Hubble types (Evrard 1989; Evrard, Silk, & Szalay 1990) or the topology of large-scale structure (Gott et al. 1989; Park & Gott 1991). Lately it has been recognized, however, that CDM models do not reproduce adequately the power spectrum at very large scales (several tens of Mpc; Ostriker 1993) and that mixed models of CDM + HDM do a significantly better job in matching the observed structures (e.g., Klypin et al. 1993, and references therein). One of the most interesting features of the CDM model concerns the idea of biased galaxy formation (Bardeen et al. 1986; Davis et al. 1985; Dekel & Silk 1986; Dekel & Rees 1987), in which normal bright galaxies which trace the large-scale structure are formed preferentially in regions of enhanced density (2–3 σ) and thus are significantly more clustered than the dark matter. On the other hand, dwarf galaxies because they originate from typical ($\sim 1\ \sigma$) density perturbations follow more closely the mass distribution and should fill in the voids seen in the bright galaxy distribution.

Several studies of the spatial distribution of dwarf galaxies were carried out to test this prediction. Most of them were based on redshift surveys of samples of low-surface-brightness (LSB) dwarfs (Bothun et al. 1986; Thuan, Gott, & Schneider 1987; Eder et al. 1989; Weinberg et al. 1991; Salzer, Hanson, & Gavazzi 1990; Binggeli, Tarenghi, & Sandage 1990; Thuan et al. 1991; Hopp 1994). All but one group found that LSB dwarfs do not fill in the voids and that they follow closely the structures delineated by bright galaxies, in contradiction with the predictions of biased galaxy formation models. On the other side, there is evidence that the clustering properties of bright normal galaxies are not identical to those of LSB dwarf galaxies. Thuan et al. (1991) found the amplitude of the two point correlation function of LSB dwarfs at $r = 1\ h^{-1}$ Mpc to be $\sim$20% smaller than that of bright galaxies. Furthermore, Salzer et al. (1990) found LSB dwarfs in the direction of the Coma cluster to be less clustered than bright galaxies, but their result was based on a dwarf sample of only 16 galaxies.

While the weight of the evidence is against finding H I-rich LSB dwarf irregulars in voids, there has been suggestion that star-forming dwarf galaxies also known as blue compact galaxies (BCGs) have been found in voids. Salzer (1989) found

© American Astronomical Society • Provided by the NASA Astrophysics Data System

1995ApJ...443..499P

several BCGs from the University of Michigan objective prism survey in voids. Redshift surveys in the direction of one of the largest voids known, that in Bootes (Tifft et al. 1986; Moody et al. 1987; Weistrop 1989, 1994; Weistrop & Downs 1988; Weistrop et al. 1992) have revealed some two dozen emission-line galaxies, most of which are BCGs and starburst galaxies. If the presence of BCGs in voids is confirmed, this would have important consequences on theories of biased galaxy formation. BCGs are usually thought to be LSB dwarfs which are undergoing a burst of star formation. If the spatial distribution of these two classes of dwarf galaxies is shown to be different, then the above evolutionary connection would have to be rethought. Moreover, the spatial distribution of dwarf galaxies can give information on their formation processes. In CDM models, bright massive galaxies are formed in a hierarchical process by merging of dwarf galaxies. In this scheme, surviving dwarf galaxies would be found at the periphery of dense groups and clusters, and thus would show less clustering than bright galaxies. On the other hand, it has also been proposed that dwarf galaxies are the left-over debris from interactions and mergers of massive galaxies at comparatively late epochs ($z \sim 1$) (Lacey & Silk 1991; Mirabel, Lutz, & Maza 1991; Mirabel, Dottori, & Lutz 1992; Barnes 1992). In this case, the spatial distribution of dwarf galaxies should follow closely that of bright galaxies.

With those considerations in mind, we have undertaken the study of the spatial distribution of a new large sample of BCGs discovered in the Second Byurakan Survey (SBS). In § 2, we discuss the SBS BCG sample and some of its statistical properties. Section 3 discusses the sample of bright galaxies taken from the Center for Astrophysics (CfA) galaxy survey, to which the SBS BCG sample will be compared. In § 4, we discuss the completeness of the SBS BCG sample and use the distance to the nearest bright neighbor statistic to analyze the spatial distribution of BCGs relative to that of bright galaxies. Section 5 focuses on the group of BCGs which do not have a companion within 5 Mpc and which lie in the voids delineated by the bright galaxy distribution. Section 6 discusses the implications of the results obtained for the dwarf spatial distribution on models of dwarf galaxy formation and evolution. We summarize our findings in § 7. Throughout this paper, h denotes the Hubble constant in units of 100 km s^{-1} Mpc^{-1}.

2. THE BLUE COMPACT GALAXY SAMPLE

Our BCG sample was primarily assembled from objective prism survey plates obtained with the 1 m Schmidt telescope at the Byurakan Observatory of the Armenian Academy of Sciences during the Second Byurakan Survey (SBS; Markarian, Lipovetsky, & Stepanian 1983; Stepanian et al. 1987). The objective prism plates cover the sky region defined by $7^h40^m \leq \alpha \leq 17^h20^m$, $49° \leq \delta \leq 61.°2$, an area of about 1000 square degrees. All objects with prism spectra showing strong or moderate emission lines were observed spectroscopically with the 6 m telescope of the Special Astrophysical Observatory with a spectral resolution of ~13 Å. We then select all emission-line galaxies with a H II region-like spectrum (i.e., showing a narrow [O III] 5007 Å line) to constitute our BCG sample. The above criterion allowed us to exclude massive nuclear starburst galaxies and galaxies with an active galactic nucleus such as Seyfert galaxies and quasars. In addition, we have also added ~50 BCGs from the First Byurakan Survey (Markarian et al. 1989) and a few BCGs from the Case Survey (Pesch & Sanduleak 1987), which are in the same sky area and

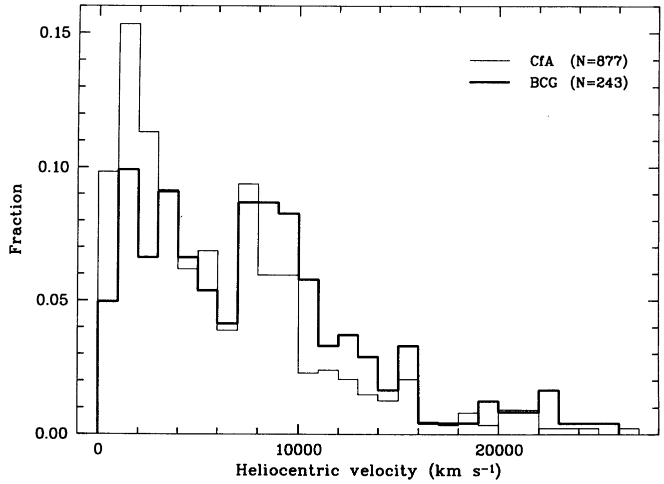

FIG. 1.—Heliocentric velocity distributions of: the Second Byurakan Survey (SBS) blue compact galaxy (BCG) sample (*thick line*) and the Center for Astrophysics (CfA) bright galaxy sample (*thin line*).

which satisfy the above criterion. The resulting sample contains a total of 243 BCGs (Izotov et al. 1992). Figure 1 shows in thick lines the normalized redshift distribution of the sample. Velocities are heliocentric. Most of the redshifts come from Stepanian et al. (1993a–d) and have an accuracy of ~50–100 km s^{-1}. More accurate optical and 21-cm velocities (accuracy ~10–20 km s^{-1}) have been taken from Izotov, Thuan, & Lipovetsky (1994), Thuan, Izotov, & Lipovetsky (1995a) and Thuan et al. (1995b). It can be seen on Figure 1 that the SBS BCG sample is reasonably complete out to ~10,000 km s^{-1}, with increasing incompleteness beyond. The velocity peak at $v \sim 1000$ km s^{-1} due to the Virgo cluster is clearly seen. There are two additional velocity peaks, at $v \sim 3000$ km s^{-1} and $v \sim 7000$–10,000 km s^{-1}. Figure 2 shows the right ascension-velocity wedge diagram for the sky region of the SBS BCG survey. The SBS BCG galaxies are shown in circles, both open and filled, the difference between the two symbols being discussed later. Figure 3 shows the projected sky distribution of the SBS BCG sample, with the BCGs in the same symbols as in Figure 2. Since we are interested in the large-scale space distribution of BCGs in this paper, we have further restricted the BCG sample to include only galaxies with heliocentric velocities larger than 2000 km s^{-1}, in order to suppress the undue influence of the Local Supercluster. We thus end up with a BCG sample containing 207 galaxies. Figures 4*a* and 4*b* show in thick lines respectively the photographic apparent and absolute magnitude distributions of the nonrestricted SBS BCG sample and Figures 4*c* and 4*d* that of the restricted sample ($v_{hel} > 2000$ km s^{-1}). The photographic apparent magnitudes are eye estimates from the Palomar Sky Survey blue prints, using objects with known photometry in the same field. Comparison with ~20 BCGs from the sample for which CCD photometry is available shows that these photographic apparent magnitudes have accuracies of ±0.5 mag. The apparent magnitude distribution (Fig. 4*a*) drops off sharply beyond $m_{pg} \sim 18$ mag, signaling an increasing incompleteness beyond that limit. As for the absolute magnitude distribution, it can be seen that the majority of the BCGs have $M_{pg} \geq -18$ and thus can be considered as dwarfs. They are in fact similar to the class of blue compact dwarfs defined by Thuan & Martin (1981). Comparison of Figures 4*b* and 4*d* shows that suppressing BCGs with $v_{hel} \leq 2000$ km s^{-1} removes the 36 faintest

© American Astronomical Society • Provided by the NASA Astrophysics Data System

1995ApJ...443..499P

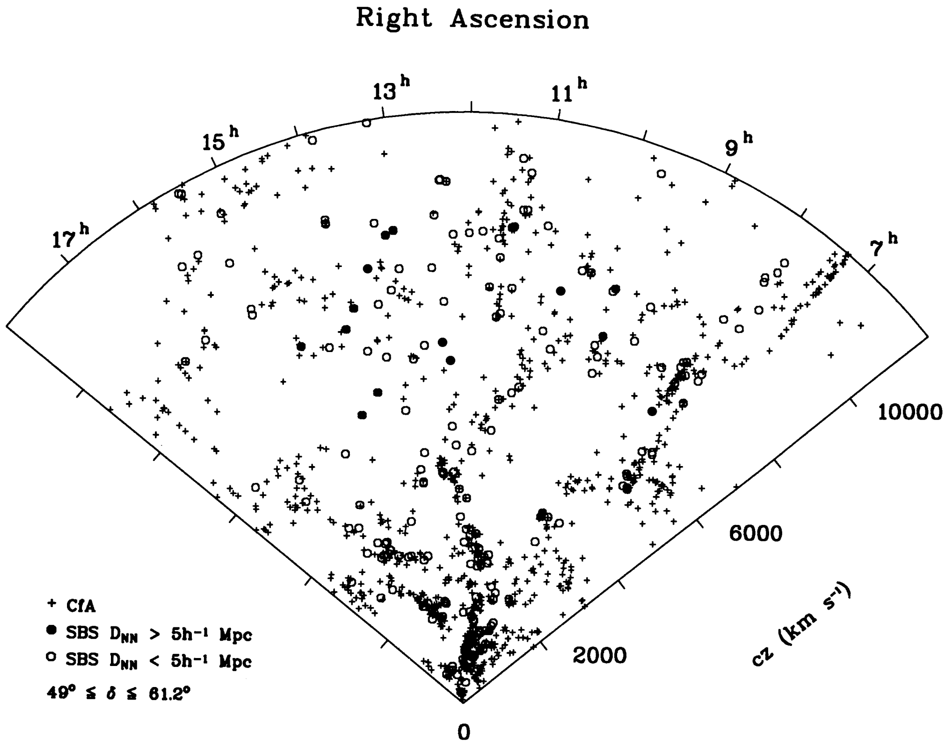

FIG. 2.—Heliocentric velocity vs. right ascension wedge diagram for the SBS zone ($49° \leq \delta \leq 61.2°$). Bright CfA galaxies are shown as crosses, SBS BCGs without a bright neighbor within $5\,h^{-1}$ Mpc are shown as filled circles, and SBS BCGs with a bright neighbor within $5\,h^{-1}$ Mpc are shown as open circles.

BCGs with $-14 \leq M_{pg} \leq -12$, but does not change appreciably the M_{pg} distribution of the SBS BCG sample.

3. THE COMPARISON BRIGHT GALAXY SAMPLE

We wish to compare the spatial distribution of BCGs in the SBS zone with that of bright galaxies in the same sky region. For the comparison bright galaxy sample we use the Center for Astrophysics (CfA) magnitude-limited ($m_B \leq 14.5$) galaxy sample (Huchra et al. 1983), a total of 877 galaxies. Figure 1 shows in thin lines the normalized redshift distribution of the CfA catalogue. Comparison with the BCG redshift distribution shows that the two distributions are very similar except for a

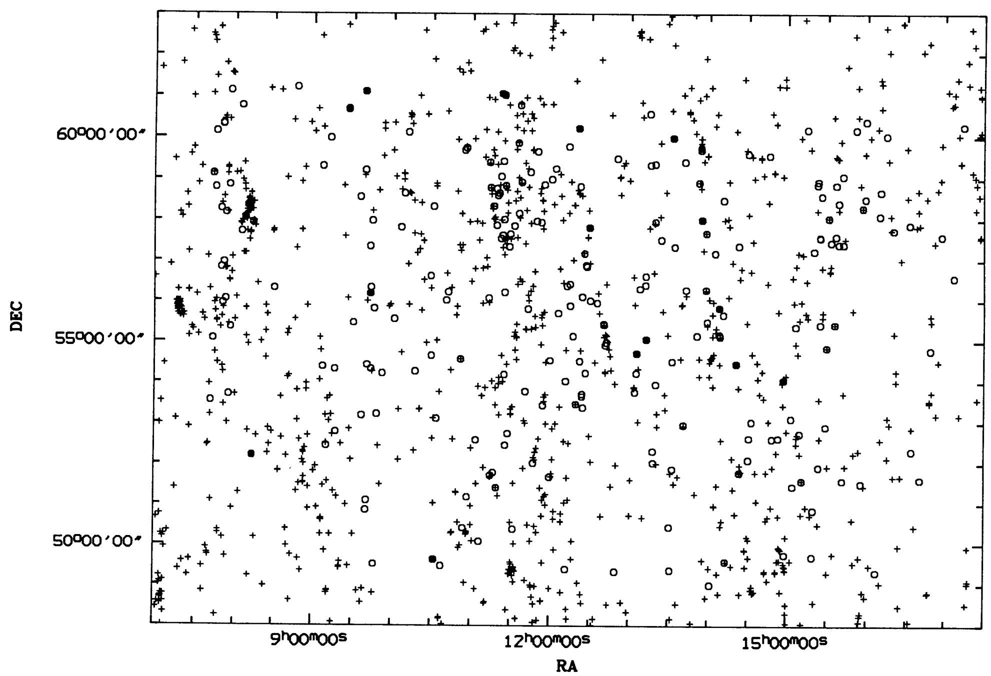

FIG. 3.—Sky projection of positions of SBS BCGs and CfA galaxies. The symbols have the same meaning as in Fig. 2

© American Astronomical Society • Provided by the NASA Astrophysics Data System

1995ApJ...443..499P

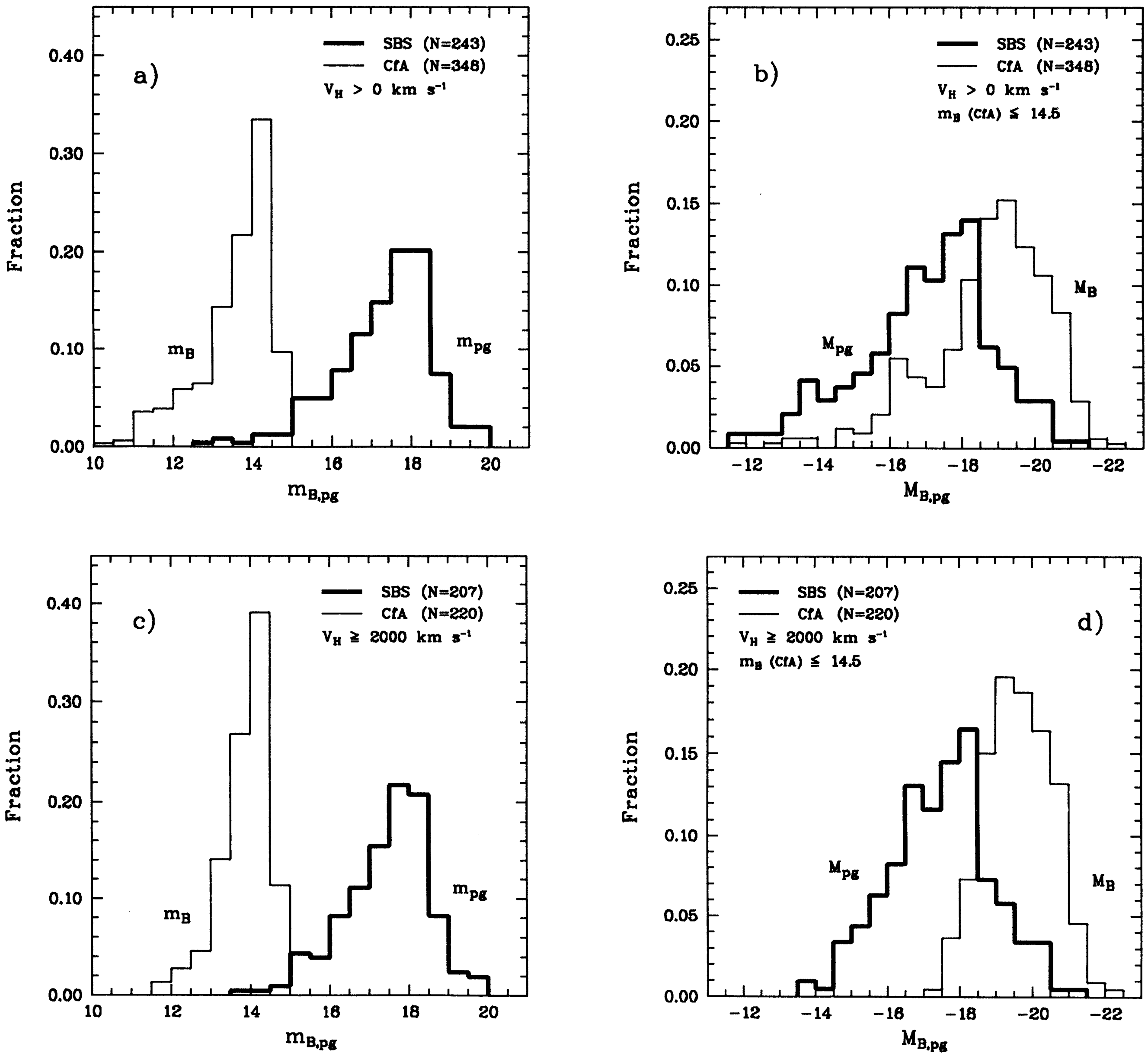

FIG. 4.—(*a*) Apparent magnitude distributions for the unrestricted SBS BCG (m_{pg}) and CfA (m_B) samples ($m_B \sim m_{pg} - 0.2$). (*b*) Absolute magnitude distributions for the unrestricted SBS BCG and CfA samples. (*c*) Apparent magnitude distributions for the SBS BCG and CfA samples restricted to galaxies with heliocentric velocities larger that 2000 km s^{-1}. (*d*) Absolute magnitude distributions for the SBS BCG and CfA samples restricted to galaxies with heliocentric velocities larger than 2000 km s^{-1}.

deficiency of BCGs relative to bright galaxies in the velocity range 0 to 3000 km s^{-1} and an excess of BCGs relative to bright galaxies in the velocity range 8000 to 10,000 km s^{-1}. The redshift distribution of the CfA galaxies drops off beyond 10,000 km s^{-1}, indicating increasing incompleteness beyond that velocity limit. The CfA galaxies are shown as crosses in the right ascension—velocity wedge diagram (Fig. 2). A cursory look at the wedge diagram shows that some BCGs (*open and filled circles*) appear to be less clustered than bright galaxies. In particular, there is a group of several BCGs at R.A. ~ 14^h and $v \sim 7000$ km s^{-1} which lie clearly in a void delineated by bright galaxies. Figure 3 shows the projected sky distribution of the CfA galaxies (*crosses*) as compared to that of BCGs (*open and filled circles*).

Figures 4*a* and 4*b* show, respectively, in thin lines the *B* apparent and absolute magnitude distributions of the CfA sample, without any velocity restriction. As expected, the SBS BCGs are generally fainter than the CfA galaxies, the peak of the absolute magnitude distribution being at $M_B \sim -18$ for the SBS BCGs, and being at $M_B \sim -19.5$ for the CfA galaxies. Figures 4*c* and 4*d* shows the same distributions for the restricted CfA sample, with galaxies with $v_{hel} \leq 2000$ km s^{-1} removed to suppress the influence of the Local Supercluster. Comparison of Figures 4*b* and 4*d* reveals that the velocity restriction cuts off the low-luminosity tail of the CfA absolute magnitude distribution at $M_B \sim -17$.

How representative is the SBS region from the point of view of large-scale structure? We can get some insight into this

© American Astronomical Society • Provided by the NASA Astrophysics Data System

1995ApJ...443..499P

TABLE 1

Clusters of Galaxies in SBS Zone

Cluster	α(1950)	δ(1950)	v_{hel}[a]	References
A569	$07^h05^m24^s$	48°43′	6050	1
Zw 286–01	07 33 24	61 02	5920	1
A634	08 10 30	58 12	8010	2
Zw 263–45	08 29 36	52 45	4830	1
Zw 265–16	09 43 42	54 54	7440	1, 2
Zw 268–11	11 38 42	56 50	2970	1
UMa	11 53 48	47 47	1360	4
Zw 292–47	12 07 36	57 35	4940	1
Zw 294–06	13 02 12	62 43	8600	1
Zw 248–14	14 56 12	49 01	4100	2, 3
Zw 276–14	16 13 48	56 32	4800	1
Zw 299–15	16 38 24	60 38	4900	1, 2
Zw 300–04	17 30 24	58 29	8530	1, 2

[a] v_{hel}: heliocentric velocity in km s^{-1}.

References.—(1) Baesi-Pillastrini et al. 1984; (2) Richter & Huchtmeier 1991; (3) Tago 1984; (4) Geller & Huchra 1983.

question by examining the maps of the large-scale distribution of galaxies by Fairall et al. (1990), based on the redshifts of more than 20,000 galaxies. We found that the region under study here is reasonably homogeneous. Apart from the presence of the Local Supercluster, there are no large-scale galaxy structure such as the Great Wall (Ramella et al. 1992) or other superclusters out to 8000 km s^{-1}. Beyond 8000 km s^{-1}, our region includes the very northern part of the Great Wall which shows up as a very dispersed structure. There are two very large voids, the centers of which are at R.A. $\sim 15^h30^m$, $v \sim 7000$ km s^{-1} and R.A. $\sim 10^h$, $v \sim 5000$ km s^{-1}. Figure 2 shows the characteristic network of filamentary structures delineating voids seen in other slices of the universe, with, at the intersection of the filaments, several known Abell clusters of richness 0 and Zwicky clusters (Baieisi-Pillastrini, Palumbo, & Vettolani 1984; Tago 1987; Richter & Huchtmeier 1991) which are listed in Table 1. We conclude that the SBS zone is fairly typical of the rest of the Universe and does not contain a large-scale inhomogeneity which would unduly bias our results.

4. THE SPATIAL DISTRIBUTION OF BLUE COMPACT GALAXIES

4.1. *Completeness of the Sample*

In order to study the large-scale clustering properties of the SBS BCG sample, we need to estimate its completeness. We do this by using the V/V_m method (Schmidt 1968; Huchra & Sargent 1973). Here V is the volume contained in a sphere with radius equal to the distance to the BCG, and V_m is the volume inside the sphere with radius equal to the maximum distance the galaxy could have and still be in the sample under study, i.e., still be brighter than the blue apparent magnitude limit m_{lim}.

The expression for V_m is then

$$V_m = \left(\frac{4\pi}{3}\right) \text{dex}\, \{0.6[m_{lim} - 25 - M_{pg} - 0.24 \operatorname{cosec}(|b^{II}|)]\} \text{ Mpc}^3 .$$

Table 2 gives the mean $\langle V/V_m \rangle$ ratio for the BCGs as a function of photographic limiting apparent magnitude in intervals of 0.5 mag, and photographic absolute magnitude in intervals of 1 mag. To derive distances, we use velocities v_{cor} which have been corrected to the centroid of the Local Group and for a Virgocentric infall velocity of 220 km s^{-1}, using the nonlinear Virgocentric flow model described by Kraan-Kortewag (1986).

The mean value $\langle V/V_m \rangle$ over the whole sample should be equal to 0.5 for objects uniformly distributed in Euclidian space if the sample is complete. Table 2 shows that $\langle V/V_m \rangle$ is close to 0.5 down to $m_{pg} = 18$. Beyond this limit, $\langle V/V_m \rangle$ drops precipitously, indicating increasing incompleteness. We shall thus adopt $m_{pg} = 18$ mag for the completeness limit of the SBS BCG sample. To avoid the effect of the Local Supercluster in our clustering analysis, we have also imposed a lower velocity cutoff of 2000 km s^{-1} to our BCG sample. An upper velocity cutoff of 8000 km s^{-1} was also set to take into account edge effects (§ 4.2). The total number of BCGs with $m_{pg} \leq 18$ mag and $2000 \leq v_{cor} \leq 8000$ km s^{-1} is 96. Table 3 gives their coordinates, apparent photographic magnitudes, heliocentric velocities, velocities corrected for Virgocentric infall and to the centroid of the Local Group and absolute photographic magnitudes. The corresponding number of CfA bright galaxies with $m_B \leq 14.5$ mag and $2000 \leq v_{cor} \leq 8000$ km s^{-1} is 155.

4.2. *Analysis of Volume-limited Subsamples*

We now attempt to quantify the visual impression provided by Figures 2 and 3 by using statistical tools to study the spatial distribution of the SBS BCGs relative to that of the CfA galaxies. We chose to use the Nearest Neighbor statistic D_{NN}, where D_{NN} is the distance of a given galaxy, be it a bright galaxy or a BCG, to its nearest neighboring bright galaxy. For the problem we want to study, whether BCGs are more uni-

TABLE 2

$\langle V/V_m \rangle$ Test[a]

Absolute Magnitude M_{pg}	Limiting Photographic Apparent Magnitude											
	14.0	14.5	15.0	15.5	16.0	16.5	17.0	17.5	18.0	18.5	19.0	19.5
−12.0	0.000(0)	0.000(0)	0.000(0)	0.000(0)	0.000(0)	0.000(0)	0.000(0)	0.000(0)	0.000(0)	0.000(0)	0.000(0)	1.000(1)
−13.0	0.000(0)	0.000(0)	0.000(0)	0.000(0)	0.000(0)	0.000(0)	0.000(0)	0.000(0)	0.000(0)	1.000(2)	0.501(2)	0.251(2)
−14.0	0.000(0)	0.000(0)	0.000(0)	0.000(0)	0.000(0)	0.000(0)	0.000(0)	1.000(2)	0.875(8)	0.501(9)	0.251(9)	0.126(9)
−15.0	0.000(0)	0.000(0)	0.000(0)	0.000(0)	0.000(0)	1.000(1)	0.834(3)	0.782(8)	0.768(21)	0.385(21)	0.263(23)	0.132(23)
−16.0	0.000(0)	0.000(0)	0.000(0)	1.000(1)	0.501(1)	0.906(8)	0.664(13)	0.458(16)	0.560(28)	0.456(37)	0.320(42)	0.160(42)
−17.0	0.000(0)	0.000(0)	0.000(0)	0.000(0)	1.000(3)	0.751(6)	0.679(13)	0.723(31)	0.466(37)	0.234(37)	0.117(37)	0.059(37)
−18.0	0.000(0)	1.000(1)	0.875(4)	0.439(4)	0.603(10)	0.535(15)	0.561(25)	0.281(25)	0.141(25)	0.071(25)	0.035(25)	0.018(25)
−19.0	0.501(1)	0.251(1)	0.563(2)	0.641(4)	0.477(6)	0.239(6)	0.120(6)	0.060(6)	0.030(6)	0.015(6)	0.008(6)	0.004(6)
−20.0	0.000(0)	0.000(0)	1.000(1)	0.501(1)	0.251(1)	0.126(1)	0.063(1)	0.032(1)	0.016(1)	0.008(1)	0.004(1)	0.002(1)
All	0.501(1)	0.626(2)	0.804(7)	0.582(10)	0.602(21)	0.604(37)	0.570(61)	0.510(89)	0.474(126)	0.304(138)	0.193(145)	0.103(146)

[a] The table gives $\langle V/V_m \rangle$. The number of galaxies on which each value is based is given in parentheses.

© American Astronomical Society • Provided by the NASA Astrophysics Data System

1995ApJ...443..499P

TABLE 3

COORDINATES, VELOCITIES, AND MAGNITUDES OF BLUE COMPACT GALAXIES IN THE SBS STATISTICAL SAMPLE[a]

SBS	α(1950)	δ(1950)	m_{pg}[b]	v_{hel}[c]	v_{cor}[d]	M_{pg}[b]
0741+535	07ʰ41ᵐ34ˢ8	+53°32′55″	17.0	5467	5684	−17.26
0743+550	07 43 10.0	+55 04 22	17.0	5493	5716	−17.27
0743+591B	07 43 32.2	+59 07 52	18.5	6340	6564	−16.06
0745+587	07 45 24.9	+58 47 09	18.0	6370	6592	−16.57
0749+568	07 49 37.7	+56 49 41	18.0	5472	5703	−16.25
0750+559	07 50 42.2	+55 56 57	16.5	7552	7749	−18.41
0753+581W......	07 53 14.4	+58 10 18	17.5	5683	5916	−16.82
0756+588	07 55 57.8	+58 50 57	16.5	5713	5948	−17.83
0756+611	07 56 29.3	+61 07 25	17.5	6269	6503	−17.02
0810+583	08 10 11.2	+58 21 05	17.0	7786	7992	−17.95
0813+522	08 13 52.6	+52 11 55	17.0	7246	7259	−17.73
0847+612	08 47 25.0	+61 12 33	16.6	4139	4424	−17.02
0912+599	09 12 53.5	+59 58 53	15.6	4150	4437	−18.00
0917+527	09 17 25.7	+52 46 53	17.0	2297	2628	−15.45
0926+606	09 26 20.1	+60 40 02	17.5	4100	4393	−16.07
0926+607	09 26 22.5	+60 41 15	18.0	4190	4481	−15.61
0935+585	09 35 36.5	+58 33 14	18.0	7200	7432	−16.70
0936+531	09 36 51.2	+53 10 56	18.0	7547	7759	−16.78
0940+544	09 40 50.4	+54 25 28	18.0	1733	2098	−13.94
0943+543	09 43 40.8	+54 19 34	18.0	1660	2027	−13.86
0943+563	09 43 44.1	+56 20 02	17.5	7745	7965	−17.34
1011+601A	10 11 31.4	+60 06 06	17.5	2323	2688	−14.97
1011+600B	10 11 33.6	+60 03 58	17.5	2188	2559	−14.86
1028+566	10 28 55.2	+56 37 07	16.5	7411	7647	−18.22
1030+583	10 30 56.3	+58 19 20	16.5	2426	2789	−16.04
1040+560	10 40 45.0	+56 01 27	15.5	7740	7973	−19.31
1055+597	10 55 43.0	+59 45 17	18.0	6540	6803	−16.47
1057+511A	10 57 02.6	+51 10 15	14.5	2881	3219	−18.32
1057+511B	10 57 10.5	+51 07 30	17.5	3056	3386	−15.43
1103+526	11 03 35.1	+52 35 00	17.0	6402	6651	−17.40
1114+587	11 14 10.7	+58 47 24	17.5	1681	2085	−14.39
1114+517	11 14 42.6	+51 42 17	16.5	2838	3185	−16.29
1118+578B	11 18 49.5	+57 51 57	16.5	2163	2553	−15.83
1119+514	11 19 21.3	+51 24 06	17.5	6235	6488	−16.84
1124+580	11 24 35.7	+58 00 42	17.5	5809	6086	−16.71
1124+541	11 24 45.5	+54 11 26	16.5	2948	3297	−16.37
1125+562	11 25 07.3	+56 13 05	16.0	5591	5869	−18.13
1125+588	11 25 42.8	+58 50 23	13.5	3150	3498	−19.51
1125+525	11 25 50.7	+52 27 22	17.0	2797	3150	−15.77
1128+573	11 28 28.9	+57 20 34	18.5	1770	2175	−13.47
1136+607	11 36 26.4	+60 46 35	18.0	3457	3799	−15.19
1137+589	11 37 48.3	+58 55 10	18.0	1854	2261	−14.06
1144+591	11 44 21.9	+59 09 50	16.5	2830	3196	−16.31
1149+596	11 49 55.8	+59 39 37	18.0	3427	3771	−15.17
1152+579	11 52 52.1	+57 56 26	16.5	5146	5442	−17.46
1159+545	11 59 29.0	+54 32 33	18.0	3537	3872	−15.21

SBS	α(1950)	δ(1950)	m_{pg}[b]	v_{hel}[c]	v_{cor}[d]	M_{pg}[b]
1203+592	12 03 43.0	+59 15 01	17.0	3273	3625	−16.08
1205+557	12 05 57.5	+55 42 07	15.5	1838	2250	−16.54
1213+597	12 13 34.8	+59 47 03	15.6	4365	4686	−18.04
1216+551	12 16 56.0	+55 08 13	18.0	5266	5559	−16.06
1221+602	12 21 00.5	+60 13 07	18.0	6987	7260	−16.59
1221+545B	12 21 58.6	+54 31 25	18.0	5654	5939	−16.14
1222+588	12 22 29.1	+58 49 17	18.0	4722	5035	−15.79
1229+578	12 29 24.3	+57 48 36	18.0	7361	7626	−16.69
1240+554C	12 40 36.0	+55 24 59	16.5	4687	4998	−17.27
1241+549	12 41 30.2	+54 55 10	17.0	4741	5050	−16.78
1242+549	12 42 22.8	+54 59 02	16.0	4740	5049	−17.78
1249+493	12 49 35.8	+49 19 45	17.5	7330	7581	−17.16
1304+537	13 03 55.8	+53 45 33	16.0	7085	7353	−18.60
1307+563	13 07 41.5	+56 18 21	18.0	5165	5475	−15.97
1314+605	13 14 54.2	+60 34 20	18.0	2050	2468	−14.25
1317+523A	13 17 42.4	+52 19 54	16.0	4581	4895	−17.71
1317+523B	13 17 56.2	+52 18 32	16.0	4560	4875	−17.71
1318+520	13 18 07.4	+52 01 37	16.0	4844	5152	−17.83
1323+575	13 23 57.8	+57 30 39	15.0	6089	6382	−19.30
1334+573	13 34 04.9	+57 20 38	18.0	7219	7496	−16.65
1340+529	13 40 55.9	+52 57 36	16.5	1801	2226	−15.51
1341+594	13 41 44.9	+59 25 07	18.0	3073	3447	−14.97
1353+597A	13 53 56.4	+59 45 22	17.5	6571	6864	−16.97
1354+597W......	13 54 00.5	+59 42 18	18.0	3010	3387	−14.94
1422+573	14 22 57.6	+57 21 47	15.0	3171	3542	−18.04
1423+518	14 23 41.0	+51 46 44	18.0	2141	2554	−14.31
1430+596	14 30 03.2	+59 36 44	17.5	1810	2239	−14.55
1430+521	14 30 21.4	+52 06 04	17.5	7730	7998	−17.30
1430+526A	14 30 53.1	+52 37 59	17.5	3167	3533	−15.52
1446+595	14 46 20.6	+59 34 20	18.0	2121	2538	−14.33
1453+526	14 53 09.0	+52 37 54	17.0	3267	3630	−16.09
1503+531	15 03 01.9	+53 06 53	17.0	5619	5924	−17.16
1504+514N	15 04 18.3	+51 26 36	16.5	3621	3971	−16.79
1506+553	15 06 24.8	+55 22 34	15.0	3453	3813	−18.21
1509+527	15 09 31.6	+52 44 44	15.0	3608	3960	−18.29
1519+496	15 19 16.8	+49 41 34	16.0	4548	4870	−17.74
1523+519	15 23 51.6	+51 55 22	18.0	3694	4042	−15.34
1524+554	15 24 40.0	+55 25 30	17.0	3408	3770	−16.19
1533+574	15 33 04.1	+57 27 00	18.0	3390	3667	−15.14
1542+574	15 42 38.0	+57 23 52	18.0	4143	4486	−15.59
1555+515	15 55 40.2	+51 30 53	17.0	3617	3966	−16.32
1558+585	15 58 54.8	+58 31 11	18.0	4242	4584	−15.65
1634+523	16 34 07.9	+52 18 57	16.5	2710	3086	−16.31
1707+565	17 07 03.3	+56 34 34	17.0	3339	3697	−16.24
1714+602	17 14 23.0	+60 16 15	16.5	6090	6395	−17.95

[a] Only 91 out of the 96 BCGs in the SBS statistical sample ($2000 \le v_{cor} \le 8000$ km s^{-1}, $m_{pg} \le 18$ mag, $7^h40^m \le \alpha \le 17^h20^m$, $49° \le \delta \le 61.°2$) are listed here. The data for the remaining five BCGs (0916+543, 1159+516B, 1212+493, 1358+554E, 1551+602A) will be given elsewhere.
[b] Photographic magnitudes are eye estimates from the Palomar Sky Survey prints and are accurate to ±0.5 mag.
[c] v_{hel}: heliocentric velocity.
[d] v_{cor}: velocity corrected to the centroïd of the Local Group and for a Virgo infall velocity of 220 km s^{-1} (Kraan-Korteweg 1986).

formly distributed than bright galaxies and whether they are in voids, the D_{NN} statistic appears to be more appropriate than the more widely used statistical measure of large-scale clustering, the correlation function.

In order to be sure that the conclusions we arrive at are not affected by selection effects, we first extract from our complete statistical ($m_{pg} \le 18$ mag) several volume-limited subsamples. While the use of subsamples sacrifices statistics, it has the advantage of eliminating the problem of selection functions.

We consider the nine volume-limited subsamples listed in Table 4. Column (2) gives the velocity range. Each subsample begins at 2000 km s^{-1}, to avoid the effect of the Local Supercluster, and cuts off at an upper velocity limit. This upper limit goes up by increments of 500 km s^{-1}. The M_{pg}^{lim} corresponding to this upper velocity limit and $m_{pg} = 18$ mag is given in column (3). Columns (4) and (5) give, respectively, the number of BCGs in each subsample, with and without removal of the clusters listed in Table 1 (see § 4.4). The corresponding M_B^{lim} (the CfA sample is magnitude-limited at $m_B = 14.5$ mag) and numbers for the CfA galaxies with and without removal of the clusters listed in Table 1 are given in columns (6), (7), and (8). We note that, although each successive subsample fills an increasingly larger volume of space, the number of galaxies in each subsample does not increase significantly, but even decreases as in the case of the CfA sample. This is due to the combined effects of the increasingly brighter lower absolute magnitude limit M_B^{lim} or M_{pg}^{lim} and the shape of the galaxian luminosity function which is such that there is progressively

© American Astronomical Society • Provided by the NASA Astrophysics Data System

1995ApJ...443..499P

TABLE 4

PARAMETERS OF VOLUME-LIMITED COMPLETE SUBSAMPLES

SUBSAMPLE (1)	VELOCITY RANGE ($km\ s^{-1}$) (2)	SBS BCGs M_{pg}^{lim} (3)	N_1[a] (4)	N_2[b] (5)	BRIGHT GALAXIES M_B^{lim} (6)	N_1[a] (7)	N_2[b] (8)
1..........	2000–4000	−15.01	24	28	−18.51	61	66
2..........	2000–4500	−15.27	29	33	−18.77	61	70
3..........	2000–5000	−15.49	30	34	−18.99	60	72
4..........	2000–5500	−15.70	29	34	−19.20	59	72
5..........	2000–6000	−15.89	35	39	−19.39	59	72
6..........	2000–6500	−16.06	36	40	−19.56	49	58
7..........	2000–7000	−16.23	36	40	−19.73	40	48
8..........	2000–7500	−16.38	36	38	−19.88	40	46
9..........	2000–8000	−16.52	43	46	−20.02	39	45

[a] Number of galaxies in subsamples with clusters removed.
[b] Number of galaxies in subsamples including clusters.

TABLE 5

KOLMOGOROV-SMIRNOV TEST AND 2 × 2 CONTINGENCY TABLE ANALYSIS OF D_{NN} DISTRIBUTION OF BLUE COMPACT GALAXIES AND BRIGHT GALAXIES

Subsample	K − S test[a] P[c]	2 × 2 Table[a] P[c]	2 × 2 Table[a] $D_{NN,th}$[d]	K − S test[b] P[c]	2 × 2 Table[b] P[c]	2 × 2 Table[b] $D_{NN,th}$[d]
1..........	0.982	0.999	2.2	0.986	1.000	2.2
2..........	0.998	0.999	2.2	0.999	1.000	2.2
3..........	0.998	0.999	2.2	0.998	1.000	1.6
4..........	0.970	0.999	1.6	0.945	0.999	1.0
5..........	0.824	0.998	1.0	0.943	0.998	1.0
6..........	0.960	0.999	2.6	0.971	0.999	2.6
7..........	0.989	0.999	2.6	0.991	0.999	2.6
8..........	0.984	0.999	2.6	0.995	1.000	2.6
9..........	0.965	0.999	2.6	0.991	1.000	2.6

[a] Without clusters.
[b] With clusters.
[c] Confidence level at which the null hypothesis that BCGs and bright galaxies have the same D_{NN} distribution is rejected.
[d] Threshold nearest neighbor distance at which the null hypothesis that BCGs and bright galaxies have the same D_{NN} distribution is rejected at the highest confidence level by the 2 × 2 contingency table analysis.

less galaxies per magnitude bin as luminosity increases. These effects are more important for the CfA sample than for the BCG sample because the slope of the galaxian luminosity function is steeper in the absolute magnitude range from −18.5 to −20.0 than in the −15.0 to −16.5 range.

Although both SBS BCG and CfA samples are reasonably complete out to $v \sim 10{,}000\ km\ s^{-1}$ (see the redshift distribution of both samples in Fig. 1), we have not extended our D_{NN} analysis all the way to that velocity in order to take into account edge effects. We stop at 8000 $km\ s^{-1}$, leaving a margin of 2000 $km\ s^{-1}$ equivalent to a distance of 20 h^{-1} Mpc. Furthermore, in computing D_{NN} we have also enlarged the sky region for the bright CfA galaxies relative to the SBS BCG sample. The boundaries for the former are defined by $6^h30^m \leq \alpha \leq 18^h30^m$ and $40° \leq \delta \leq 70°$ as compared to $7^h40^m \leq \alpha \leq 17^h20^m$ and $49° \leq \delta \leq 61.2°$ for the SBS BCG sample. We note that the enlarged CfA sample is only used in calculating D_{NN}. For comparison with the BCG sample, the nonextended CfA sample, occupying the same sky area as the BCG sample, is used.

The normalized histograms of the distance D_{NN} to the nearest bright neighbor for each of the nine subsamples are given in Figure 5, both for the SBS BCG (*thick line*) and CfA galaxies (*thin line*). We have also shown in dashed lines the corresponding histograms for a random distribution of galaxies, based on the average of 100 Monte Carlo simulations.

In order to improve the statistics, we have also shown in Figure 6*a* the average normalized histogram for the five subsamples extending out the furthest in velocity (subsamples 5 to 9) and in Figure 6*b* the average normalized histogram for all nine subsamples. Examination of both Figures 6*a* and 6*b* prompts several remarks. As expected, the histograms of both galaxy samples are very different from that for a random distribution. The CfA sample shows a large excess of galaxies at small D_{NN} (0–2 h^{-1} Mpc) and a deficiency of galaxies at larger separations (2–8 h^{-1} Mpc). The histogram of the SBS BCG sample shows a large deficiency of galaxies at very small D_{NN} (0–1 h^{-1} Mpc), in agreement with the random distribution. There is then an excess of BCGs for $1 \leq D_{NN} \leq 3\ h^{-1}$ Mpc, a deficiency for $4 \leq D_{NN} \leq 6\ h^{-1}$ Mpc, and then a roughly similar distribution to a random one for $D_{NN} \geq 6\ h^{-1}$ Mpc. If we compare the histograms of the CfA and SBS BCG samples to each other, the main features to be noticed are a deficiency of BCGs relative to bright galaxies for $D_{NN} \lesssim 2\ h^{-1}$ Mpc and an excess for $D_{NN} \geq 5\ h^{-1}$ Mpc. These general trends can be also seen individually for each subsample (Fig. 5). Using the Kolmogorov-Smirnov test, we show in Table 5 that the D_{NN} distribution for BCGs and bright galaxies differs at a significance level varying between 0.943 and 0.999 for each of the nine volume-limited subsamples.

4.3. *Contingency Table Analysis*

While the Kolmogorov-Smirnov test can tell us that two given distributions of parameters differ, it cannot give us information on the range of variables (D_{NN} here) where the difference is most pronounced. Analysis of 2 × 2 contingency tables can provide that information. The contingency table method is described in detail in the Appendix. Briefly, it allows us to check whether two properties, X and Y, of objects in a sample are correlated or not. The total sample is split into four subsamples. Subsample 1 contains a_{11} members with both X and Y properties, subsample 2 contains a_{12} members with property X but without property Y, subsample 3 contains a_{21} members with property Y and without property X and subsample 4 contains a_{22} members without property X nor Y.

For the problem of concern here, property X is that of being a BCG while property Y is that of having a bright companion within a threshold value of D_{NN} (which can be varied). We consider BCGs and bright galaxies to be part of the same statistical sample. For each volume-limited subsample listed in Table 4, we have constructed several 2 × 2 contingency tables, with different threshold values of D_{NN} in h^{-1} Mpc. We show these contingency tables in Table 6 for the subsamples with the clusters removed (see § 4.4). For each table, we have given the confidence level P (the calculation of which is described in the Appendix) at which the tables are significant. Equivalently, $p = (1 - P)$ is the probability that the property X of being a BCG is independent from the property Y of having a bright companion within a threshold D_{NN}. This method is more powerful than the Kolmogorov-Smirnov test since comparison with Table 5 shows that in most cases, the significance level of the 2 × 2 contingency tables is better than that given by the Kolmogorov-Smirnov test. In addition, the method allows the study of the variation of the significance level as a function of the threshold value of D_{NN}.

© American Astronomical Society • Provided by the NASA Astrophysics Data System

1995ApJ...443..499P

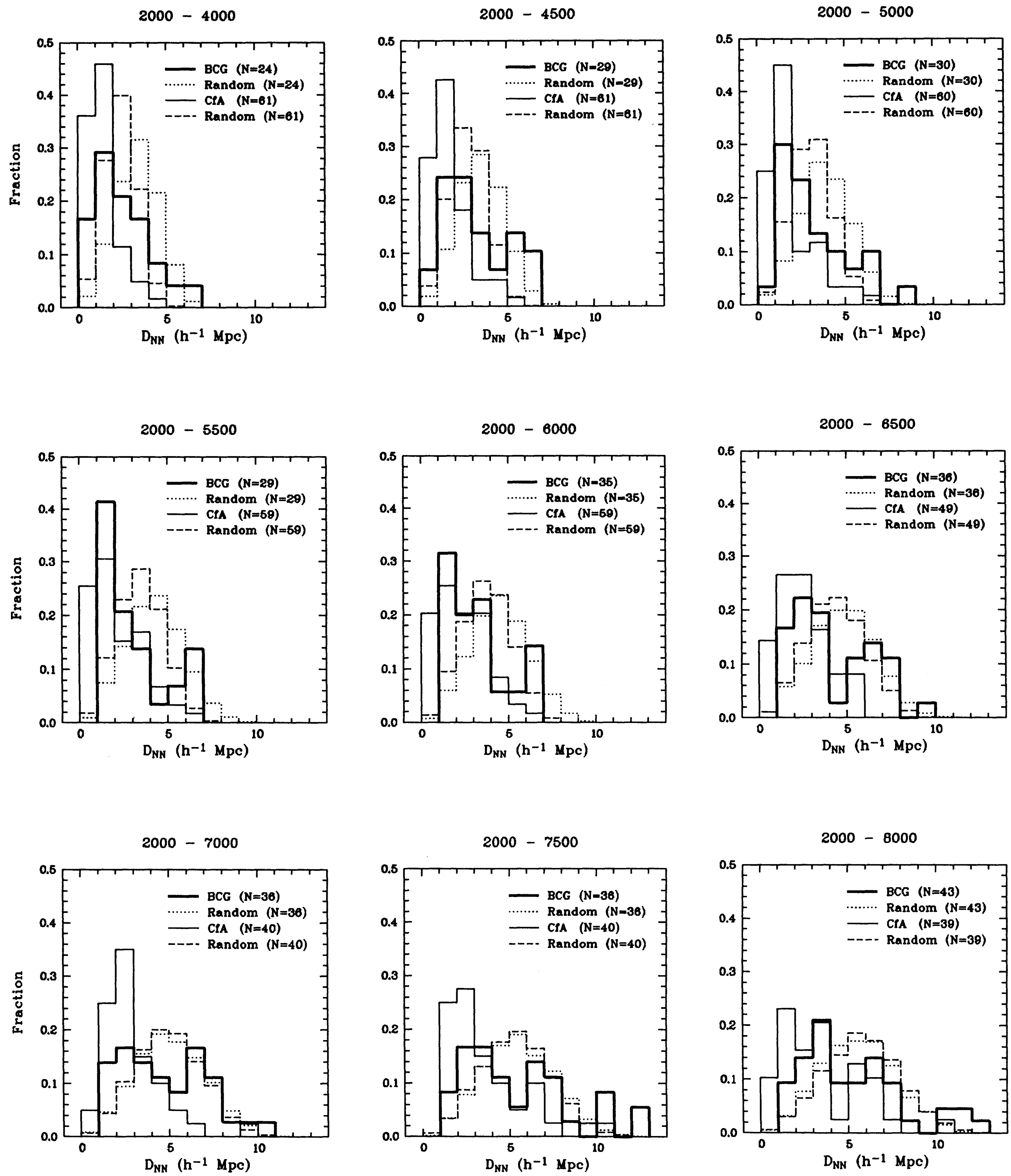

FIG. 5.—Histograms of the distribution of the distance D_{NN} to the nearest bright neighbor for all nine BCG subsamples listed in Table 4 and with clusters removed (*thick line*) and for the corresponding CfA bright galaxy subsamples (*thin line*). The histograms for the corresponding random distributions based on the average of 100 Monte Carlo simulations for both BCG and CfA subsamples are also shown in dashed lines.

© American Astronomical Society • Provided by the NASA Astrophysics Data System

1995ApJ...443..499P

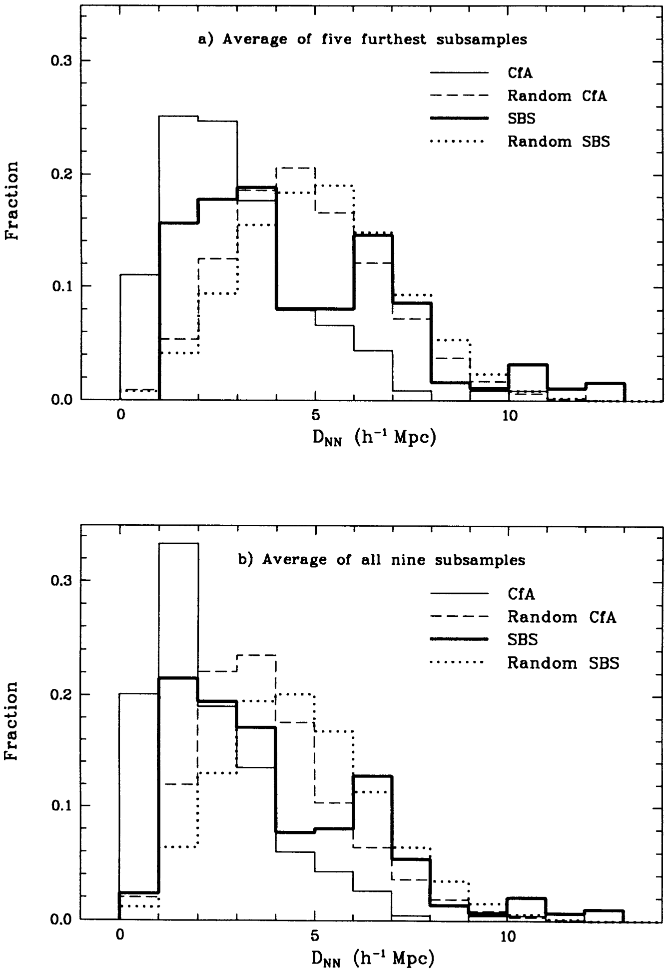

FIG. 6.—(*a*) Average of the D_{NN} histograms in Fig. 5 of the five furthest BCG and CfA subsamples with clusters removed. The mean D_{NN} for the BCG sample is 4.6 h^{-1} Mpc while that for the CfA sample is 2.9 h^{-1} Mpc. The average random distributions are also shown. The mean D_{NN} for the average random distribution corresponding to the BCG subsamples is 5.1 h^{-1} Mpc while that corresponding to the CfA subsamples is 4.7 h^{-1} Mpc; (*b*) Average of the D_{NN} histograms in Fig. 5 of all nine BCG and CfA subsamples with clusters removed. The mean D_{NN} for the BCG sample is 4.0 h^{-1} while that for the CfA sample is 2.3 h^{-1} Mpc. The average random distributions are also shown. The mean D_{NN} for the average random distribution corresponding to the BCG subsamples is 4.6 h^{-1} Mpc while that corresponding to the CfA subsamples is 3.8 h^{-1} Mpc.

4.4. *Results*

As noted before, the region under analysis contains several relatively poor clusters. We identify 2 Abell clusters of richness 0 (A569 and A634) and 11 Zwicky clusters (Table 1). These clusters may affect the distribution of D_{NN} and we remove them to make sure that any difference found in the D_{NN} distribution between bright galaxies and BCGs cannot be attributed to a morphological segregation effect. We remove all galaxies within two cylinders, both centered on the position and redshift of each cluster, one with length 1600 km s^{-1} and radius 1.3 h^{-1} Mpc to take into account the core galaxy population, and one with length 400 km s^{-1} and radius 2.6 h^{-1} Mpc to take into account the halo galaxy population. By doing so, we suppress 21 bright CfA galaxies and 13 BCGs. Examination of Table 5 shows that removal of galaxies in the vicinity of clusters does decrease slightly the confidence level at which the Kolmogorov-Smirnov test can distinguish the D_{NN} distributions of BCGs and bright galaxies, for some volume-limited subsamples (for example subsample 5). However, to discuss the results, we shall mainly make use of the 2 × 2 contingency table analysis which is more powerful than the Kolmogorov-Smirnov test in the sense that it also gives information on the range of D_{NN} where the distributions are most different.

From examination of the D_{NN} distributions (Figs. 5 and 6) and of Table 6, we have arrived at the following results:

1. There is significant (the confidence level varies from 0.950 to 0.999) deficiency of BCGs in comparison with bright galaxies for $D_{NN} \lesssim 2\ h^{-1}$ Mpc.

2. Nearly all volume-limited BCG subsamples show a clear excess in comparison with bright galaxies for $D_{NN} \gtrsim 5$ Mpc. For the four most distant BCG subsamples, this relative excess is established at a confidence level varying from 0.950 to 0.995.

3. The deficit of BCGs at $D_{NN} \lesssim 2\ h^{-1}$ Mpc is not a consequence of their excess at $D_{NN} \gtrsim 5\ h^{-1}$ Mpc. We establish this by removing from all subsamples those BCGs with $D_{NN} > 5\ h^{-1}$ Mpc. The 2 × 2 contingency table analysis applied to the remaining galaxies gives again a significant (the confidence level varies from 0.950 to 0.999) deficit of BCGs for $D_{NN} \lesssim 2\ h^{-1}$ Mpc.

4. While the D_{NN} distribution for bright galaxies shows a maximum below the mean value of D_{NN}, at $D_{NN} \sim 2\ h^{-1}$ Mpc, and a tail which extends to approximately 3 times the mean value, the D_{NN} distribution for BCGs is quite different, showing a broad peak at $1 \lesssim D_{NN} \lesssim 4\ h^{-1}$ Mpc and a distinct second peak at D_{NN} = 6–7 h^{-1} Mpc (Fig. 6). If we consider, for example, the average of the five most distant subsamples (Fig. 6*a*) then the normalized value of the D_{NN} histogram in the bins 4–6 h^{-1} Mpc is 0.08 ± 0.01, significantly less (at the 4 σ level) than the value of 0.14 ± 0.01 in the bin 6–7 h^{-1} Mpc. Thus from the point of view of their spatial distribution, there appear to be two groups of BCGs: a first group with $D_{NN} \geq 5\ h^{-1}$ Mpc constituting about 20 percent of the total in very low-density regions devoid of bright galaxies, and a second group with $D_{NN} \lesssim 5\ h^{-1}$ Mpc constituting about 80% of the total which follows closely the bright galaxy distribution but whose members are systematically at larger distances from bright galaxies than bright galaxies are from each other.

5. BLUE COMPACT GALAXIES IN VOIDS

We now discuss in more detail the BCG group in low-density environments with $D_{NN} > 5\ h^{-1}$ Mpc. This threshold value for D_{NN} is the same as that used by Salzer (1989) to identify BCGs in voids and is equal to about half the smallest void diameter seen (Kaufmann & Fairall 1991). In the SBS zone, for the velocity range $v_{hel} \leq 10{,}000$ km s^{-1} where both the SBS BCG and CfA samples are reasonably complete (Fig. 1), we have found 18 BCGs with $D_{NN} > 5\ h^{-1}$ Mpc. They are listed in Table 7, along with their coordinates, apparent and absolute photographic magnitudes, v_{cor} and D_{NN} and represented as filled circles in Figures 2 and 3. To check for the environment of these BCGs, we have used redshifts not only from J. Huchra's redshift catalogue (ZCAT, version 1990), but also from recent redshift lists from Bottinelli et al. (1993) and Schneider et al. (1990, 1992). Careful inspection of the three dimensional distribution of galaxies shows that the BCGs listed in Table 7 do indeed lie in voids delineated by the bright galaxy distribution. To illustrate this, we have shown in Figure 7 the environment of five of the most isolated BCGs in Table 7, by displaying from left to right four successive layers of 3 h^{-1}

© American Astronomical Society • Provided by the NASA Astrophysics Data System

1995ApJ...443..499P

TABLE 6

2 × 2 Contingency Tables for Volume-limited Subsamples

Subsample 1 ($V \leq 4000$ km s^{-1})										
$D_{NN,th}$[a] (h^{-1} Mpc)......	<1.0	>1.0	<1.6	>1.6	<2.2	>2.2	<6.0	>6.0	<6.4	>6.4
BCG number...........	4	20	10	14	11	13	23	1	23	1
CfA number............	22	39	46	15	52	9	61	0	61	0
P[b].....................	0.934		0.996		0.999		0.717		0.717	
Subsample 2 ($V \leq 4500$ km s^{-1})										
$D_{NN,th}$[a] (h^{-1} Mpc)......	<1.0	>1.0	<1.6	>1.6	<2.2	>2.2	<6.0	>6.0	<6.4	>6.4
BCG number...........	2	27	8	21	9	20	26	3	28	1
CfA number............	17	44	39	22	46	15	61	0	61	0
P[b].....................	0.982		0.999		0.999		0.968		0.677	
Subsample 3 ($V \leq 5000$ km s^{-1})										
$D_{NN,th}$[a] (h^{-1} Mpc)......	<1.0	>1.0	<1.6	>1.6	<2.2	>2.2	<6.0	>6.0	<6.4	>6.4
BCG number...........	1	29	6	24	10	20	26	4	28	2
CfA number............	15	45	39	21	44	16	59	1	60	0
P[b].....................	0.992		0.999		0.999		0.959		0.890	
Subsample 4 ($V \leq 5500$ km s^{-1})										
$D_{NN,th}$[a] (h^{-1} Mpc)......	<1.0	>1.0	<1.6	>1.6	<2.2	>2.2	<6.0	>6.0	<6.4	>6.4
BCG number...........	0	29	4	25	12	17	25	4	27	2
CfA number............	15	44	29	30	38	21	58	1	58	1
P[b].....................	0.999		0.999		0.965		0.961		0.747	
Subsample 5 ($V \leq 6000$ km s^{-1})										
$D_{NN,th}$[a] (h^{-1} Mpc)......	<1.0	>1.0	<1.6	>1.6	<2.2	>2.2	<6.0	>6.0	<6.4	>6.4
BCG number...........	0	35	4	31	11	24	30	5	32	3
CfA number............	12	47	22	37	32	27	58	1	59	0
P[b].....................	0.998		0.995		0.974		0.974		0.951	
Subsample 6 ($V \leq 6500$ km s^{-1})										
$D_{NN,th}$[a] (h^{-1} Mpc)......	<1.0	>1.0	<1.6	>1.6	<2.2	>2.2	<6.0	>6.0	<6.4	>6.4
BCG number...........	0	36	3	33	6	30	26	10	29	7
CfA number............	7	42	17	32	25	24	49	0	49	0
P[b].....................	0.983		0.996		0.999		0.999		0.998	
Subsample 7 ($V \leq 7000$ km s^{-1})										
$D_{NN,th}$[a] (h^{-1} Mpc)......	<1.0	>1.0	<1.6	>1.6	<2.2	>2.2	<6.0	>6.0	<6.4	>6.4
BCG number...........	0	36	2	34	5	31	23	13	27	9
CfA number............	2	38	11	29	16	24	38	2	39	1
P[b].....................	0.724		0.989		0.990		0.999		0.996	
Subsample 8 ($V \leq 7500$ km s^{-1})										
$D_{NN,th}$[a] (h^{-1} Mpc)......	<1.0	>1.0	<1.6	>1.6	<2.2	>2.2	<6.0	>6.0	<6.4	>6.4
BCG number...........	0	36	1	35	3	33	21	15	24	12
CfA number............	0	40	9	31	14	26	33	7	36	4
P[b].....................	...		0.989		0.995		0.981		0.987	
Subsample 9 ($V \leq 8000$ km s^{-1})										
$D_{NN,th}$[a] (h^{-1} Mpc)......	<1.0	>1.0	<1.6	>1.6	<2.2	>2.2	<6.0	>6.0	<6.4	>6.4
BCG number...........	0	43	2	41	4	39	27	16	31	12
CfA number............	4	35	12	27	15	24	33	6	37	2
P[b].....................	0.952		0.998		0.998		0.977		0.996	

[a] Threshold nearest neighbor distance.

[b] Confidence level at which the null hypothesis that BCGs and bright galaxies have the same D_{NN} distribution is rejected.

Mpc height, displaced in the vertical direction. The BCG of concern is shown by a cross at the center of the two central layers. Other BCGs in the field are also marked by crosses, while galaxies with $M_B \geq -18.5$ are shown as open circles and bright galaxies with $M_B < -18.5$ are show as filled circles. Examination of Figure 7 shows that these BCGs do lie in very low-density environments. Figure 2 shows that they populate voids of varying size. For example, the close pair of BCGs 0926+606 and 0926+607 ($\Delta v = 88$ km s^{-1} and a projected separation of 19 h^{-1} kpc) and 0813+522 all lie near the outskirts of the very large (diameter ~ 50 h^{-1} Mpc) Ursa Major void (Fairall 1992). The BCGs 1353+597A and 1420+540 are located in the central part of the very large (diameter ~ 50 h^{-1} Mpc) Corona Borealis void. The BCGs 1221+602 and 1229+578 lie in an intermediate-size void (diameter $\gtrsim 15$ h^{-1} Mpc) while 0938+611 and 0943+561 lie in small (diameter ~ 10 h^{-1} Mpc) voids. Many other voids remain empty of all types of galaxies. Salzer (1989) and Pustil'nik, Ugryumov, &

© American Astronomical Society • Provided by the NASA Astrophysics Data System

1995ApJ...443..499P

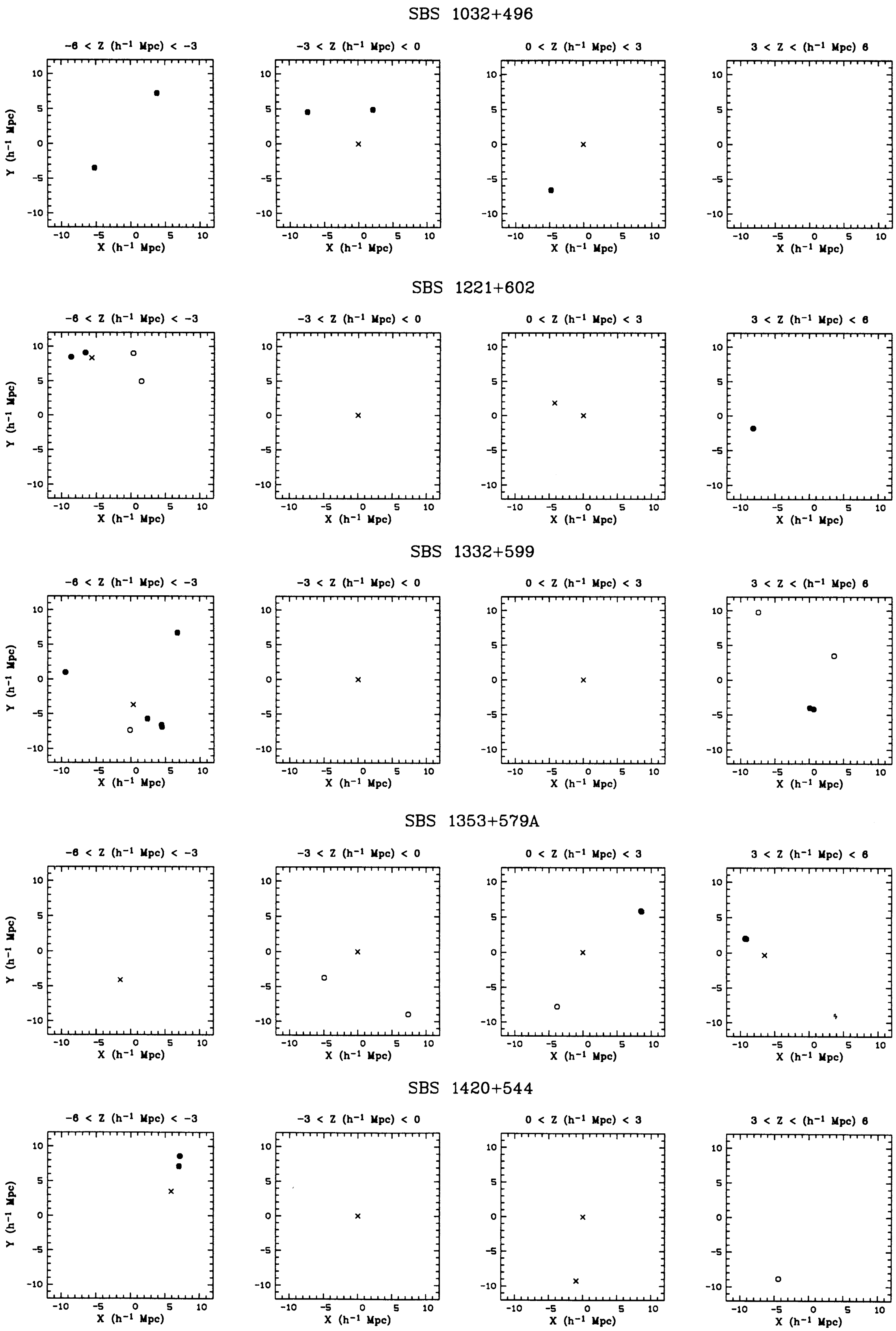

FIG. 7.—Environment of several BCGs with $D_{NN} > 5\ h^{-1}$ Mpc and which lie in voids (Table 7). For each BCG, four successive layers are shown, of 3 h^{-1} Mpc height and of 22 × 22 Mpc base, displaced vertically by 3 h^{-1} Mpc. The BCG of interest is marked by a cross in the center of the two central layers. Other BCGs are also marked by crosses, while galaxies with $M_B \geq -18.5$ are shown as open circles and bright galaxies with $M_B < -18.5$ are shown as filled circles.

© American Astronomical Society • Provided by the NASA Astrophysics Data System

1995ApJ...443..499P

TABLE 7

BLUE COMPACT GALAXIES IN VOIDS

Object	α(1950)	δ(1950)	m_{pg}	v_{cor}[a] (h^{-1} Mpc)	D_{NN}[b] (km s^{-1})	M_{pg}
0813+522	08h13m52.6	+52°11′55″	17.0	7259	5.7	−17.7
0926+606	09 26 20.1	+60 40 02	17.5	4393	5.7	−16.1
0926+607	09 26 22.5	+60 41 15	18.0	4481	6.1	−15.6
0938+611	09 38 54.1	+61 06 17	17.0	8208	6.5	−17.9
0943+561A	09 43 18.4	+56 10 51	19.0	9170	5.3	−16.1
1032+496	10 32 06.1	+49 37 16	17.0	8806	5.5	−18.0
1122+610	11 22 22.4	+61 03 29	18.5	9964	6.9	−16.8
1124+610	11 24 30.3	+61 01 26	17.0	9940	6.6	−18.2
1221+602	12 21 00.5	+60 13 07	18.0	7260	6.2	−16.6
1229+578	12 29 24.3	+57 48 35	18.0	7626	6.4	−16.7
1305+547	13 05 20.0	+54 42 49	15.5	9949	7.2	−19.8
1312+550	13 12 32.8	+55 03 46	15.0	9878	6.1	−20.2
1332+599	13 32 57.9	+59 59 49	17.5	9300	7.8	−17.6
1353+597A	13 53 56.4	+59 45 21	17.5	6864	6.6	−17.0
1354+579W......	13 54 41.9	+58 00 22	18.0	8601	6.6	−17.0
1408+558	14 08 05.5	+55 50 06	16.0	8242	6.5	−18.9
1420+544	14 20 59.1	+54 27 42	18.5	6513	11.0	−15.8
1457+540	14 57 11.6	+54 03 24	17.5	8240	10.8	−17.3

[a] v_{cor}: velocities corrected to the centroïd of the Local Group and for a Virgocentric infall velocity of 220 km s^{-1} (Kraan-Korteweg 1986).
[b] D_{NN}: distance to nearest neighbor.

Lipovetsky (1983) have suggested that these truly empty voids may be intrinsically different in their physical properties from voids containing BCGs. Weistrop (1994) has found that, in the case of the Bootes void, there may be even structure in the spatial distribution of the star-forming galaxies in the void. Unfortunately, with the present sample, we do not have a large enough number of BCGs within the same void to look for such structures.

6. DISCUSSION

The main result of our analysis of the BCG space distribution is that, while most of the BCGs ($\sim$80% of the total population) follow the structures delineated by the bright galaxy distribution, the remaining (20%) of the BCGs appear to be less clustered as compared to bright galaxies. Using the distance to the nearest bright neighbor D_{NN} as statistic, we found that the less clustered BCGs have $D_{NN} > 5\ h^{-1}$ Mpc and are found in voids delineated by the bright galaxy distribution. Our results are in agreement with those of Salzer (1989) and Salzer & Rosenberg (1994) who also found that $\sim$10%–20% of the BCGs in the University of Michigan objective prism survey are found in voids, and with those of Pustil'nik et al. (1994) who found similar results for BCGs in the Case objective prism survey. Iovino, Melnick, & Shaver (1988) also found that BCGs from southern hemisphere objective prism surveys are less clustered than bright galaxies.

Can these clustering results for BCGs be reconciled with those found for LSB dwarf galaxies? LSB dwarf galaxies are generally thought to be BCGs in their quiescent stages (Thuan 1985; Davies & Phillips 1989). The present burst of start formation in BCGs cannot last more $\sim 10^7$ years. After all massive stars made in the burst have died out, BCGs fade in surface brightness to become LSB dwarfs. The period of quiescence may last 2–3 × 10^9 yr (Fanelli, O'Connell, & Thuan 1988), before a new burst of star formation occurs, transforming LSB dwarfs back into BCGs. Thus if LSB dwarfs and BCGs are the same type of objects and the triggering of the burst does not depend on the environment of BCGs (this appears to be the case: starbursts in BCGs are probably triggered by stochastic cloud collisions within the galaxies), then the spatial distributions of BCGs and LSB dwarfs should be similar. If they differ, then the above evolutionary ideas would have to be revised. Bothun et al. (1986), Thuan et al. (1987, 1991), Eder et al. (1989) and Weinberg et al. (1991) all concluded that LSB dwarfs follow closely the bright galaxy distribution and do not fill in voids. However, Thuan et al. (1991) did find that the amplitude of the two point correlation function of LSB dwarfs was $\sim$20% smaller than that of bright galaxies at $r = 1\ h^{-1}$ Mpc. Careful examination of individual LSB dwarfs does reveal candidates in very low-density regions. For example, among the 58 LSB dwarfs in the CfA slice studied by Thuan et al. (1987), three are found in very low-density regions, with one being in a void of diameter $\sim$50 Mpc. In the LSB dwarf sample studied by Eder et al. (1989), there is a conspicuous object with $D_{NN} = 9\ h^{-1}$ Mpc while all other dwarfs have $D_{NN} < 6\ h^{-1}$ Mpc. Henning & Kerr (1989) and Henning (1992) found by a blind H I search one LSB dwarf in the Local Void and one in the Perseus-Pisces void. Salzer et al. (1990) found several dwarfs in the Coma void. Thus there is some observational evidence that there is a small ($\lesssim$10–20%) fraction of LSB dwarfs which are less clustered than bright galaxies and in very low-density environments. This minority LSB dwarf population which is less clustered was not readily apparent in previous large statistical studies (e.g., Thuan et al. 1991) because the statistic used, the two-point correlation function, may not be sensitive to such a minority population. The D_{NN} statistic used here is more appropriate for detecting such a population. Eder et al. (1989) did use the D_{NN} statistic, but they sampled only one void region, so their result may not be representative. We have carried out a preliminary analysis of the LSB dwarf sample of Thuan et al. (1991) using the D_{NN} statistic. We found that the D_{NN} distribution of the LSB dwarf sample also shows a significant excess at $D_{NN} \gtrsim 5\ h^{-1}$ Mpc relative to that of the bright CfA galaxies. Analysis of 2 × 2 contingency tables shows that the hypothesis that the D_{NN} distributions of the LSB dwarfs and the bright CfA galaxies are drawn from the same population can be rejected at the 99% confidence level. On the other hand, the hypothesis that the D_{NN} distributions of

© American Astronomical Society • Provided by the NASA Astrophysics Data System

1995ApJ...443..499P

the LSB dwarfs and that of SBS BCGs are drawn from the same population can be rejected only at the $\sim 50\%$ confidence level. This finding is consistent with the hypothesis that LSB dwarfs and BCGs are the same type of objects, but in different star-forming stages. A more detailed account of the comparison between the spatial distribution of LSB dwarfs and that of BCGs will be given in a separate paper.

What are the implications of our findings concerning theories of dwarf galaxy formation and evolution? The BCGs with $D_{NN} > 5\ h^{-1}$ Mpc and which are in voids appear to be the best candidates for the dwarf galaxies predicted by Dekel & Silk (1986) in their CDM model of biased galaxy formation. The purpose of biased galaxy models is to reconcile the mass density in the universe derived from dynamical measurements of galaxies ($\Omega \sim 0.1$) to the one expected from inflationary scenarios ($\Omega = 1$). The biasing models postulate that bright galaxies, because they form at the highest density peaks, trace only the light but not the mass distribution in the universe. Dekel & Silk (1986) have proposed a physical mechanism for galaxy biasing, based on the formation of diffuse dwarf galaxies through gas loss by supernova-driven winds. Although this theory is only directly relevant to dwarf ellipticals, the above authors have speculated that dwarf irregulars would have a similar distribution. It is clear from our results that the Dekel and Silk theory cannot be totally correct. While some BCGs are found in voids, they represent the minority ($\sim 20\%$). The majority ($\sim 80\%$) of BCGs are in or near the structures delineated by the bright galaxy distribution.

At least two theoretical scenarios for the origin of dwarf galaxies have been proposed:

1. Dwarf galaxies form from debris resulting from tidal interactions between massive galaxies (e.g., Lacey & Silk 1991; Barnes 1992).

2. Dwarf galaxies form from primordial density perturbations with mass scale $\sim 10^8$–$10^9\ M_\odot$ (Rees 1988).

The first scenario would predict that all dwarf galaxies would follow closely the bright galaxy spatial distribution, i.e. they would have D_{NN} less than $2\ h^{-1}$ Mpc. The large deficiency of dwarf galaxies in this D_{NN} range implies that, while a minority of dwarf galaxies may form as tidal debris, the vast majority may form according to the second scenario. In this scheme and in the case of gaussian initial density perturbations, there is coexistence of a wide spectrum of different mass scales. Massive density perturbations in regions of deeper than average gravitational potential will grow first into the nonlinear regime, capturing and tidally disrupting nearby lower mass slower growing density perturbations. Thus only those low-mass perturbations which are located at the periphery of the regions where massive galaxies are formed, will survive and develop into dwarf galaxies. This scenario would naturally explain the deficiency of BCGs with $D_{NN} \lesssim 2\ h^{-1}$ Mpc with respect to bright galaxies.

7. CONCLUSIONS

We have analyzed the space distribution of a complete statistical sample of 96 blue compact galaxies (BCGs) discovered in the Second Byurakan Survey (SBS) with $m_{pg} \leq 18$ mag, $2000 \leq v_{cor} \leq 8000$ km s^{-1}. As a statistical tool, we use the distance to the nearest bright neighbor D_{NN}.

We have arrived at the following conclusions:

1. The vast majority of BCGs ($\sim 80\%$) follow generally the large-scale space distribution of bright galaxies, although $\sim 20\%$ are found in very low-density regions, devoid of bright galaxies.

2. We found 18 BCGs in the SBS zone with $D_{NN} > 5\ h^{-1}$ Mpc and which lie in voids delineated by the bright galaxy distribution and whose diameters vary from 10 to 50 h^{-1} Mpc. These BCGs in voids constitute $\sim 20\%$ of the total sample. They may provide a partial support to the CDM theory of biased dwarf galaxy formation of Dekel & Silk (1986).

3. The large deficiency of BCGs with $D_{NN} < 2\ h^{-1}$ Mpc supports the hypothesis that the majority of BCGs originate as low-mass primordial density perturbations, but not as debris resulting from tidal interactions between massive galaxies.

4. The spatial distribution of BCGs is consistent with that found for low-surface brightness (LSB) dwarfs, supporting the idea that BCGs are LSB dwarfs undergoing intense bursts of star formation.

We wish to thank J. A. Stepanian and L. K. Erastova for their collaboration in assembling the SBS BCG sample, and Yu. I. Izotov, A. Yu. Kniazev, and S. N. Neizvestny for their help with the 6 m telescope observations. J. P. Huchra kindly provided us with a tape version of the CfA catalog. Thanks are due to V. S. Lebedev who provided us with the list of clusters. We had useful conversations with G. I. Beskin, A. G. Doroshkevich, and A. I. Kopylov. S. A. I. and A. V. U. thank ESO for, respectively, a C&EE Travel grant no. B0247 and Fellowship no. B03001. T. X. T. thanks the financial support of Air Force grant AFOSR 89-0467, the University of Paris VII and the Commissariat à l'Energie Atomique. This international collaboration was made possible by the award of the 1992 Henri Chrétien Award by the Americal Astronomical Society and of NATO collaborative research grant no. 921285. S. A. P., A. V. U., and T. X. T. thank Chantal Balkowski for her hospitality in the Departement d'Astronomie Extragalactique et de Cosmologie at the Observatoire de Meudon. T. X. T. thanks Laurent Vigroux for welcoming him in the Service d'Astrophysique at Saclay.

APPENDIX

THE 2 × 2 CONTINGENCY TABLE TEST

The significance test in a 2×2 contingency table is a powerful method to examine whether two physical properties of objects in a sample are correlated with each other, without knowing the precise character of the correlation. We give here a brief summary of the method with the relevant references.

Let there be a sample of N elements, divided into two subgroups 1 and 2 containing respectively n elements with property Z and $N - n$ elements without property Z. Let there be M elements in the whole sample with property Y and $N - M$ elements without property Y. Let there be m elements with both properties Y and Z. The result of dividing the total sample according to properties Y and Z is shown in the 2×2 contingency Table A1.

© American Astronomical Society • Provided by the NASA Astrophysics Data System

1995ApJ...443..499P

In the case when the division of the sample into two subgroups with and without property Z is done randomly and independently of property Y, the mathematical expectation ME of m is

$$ME(m) = \frac{nM}{N} .$$

And consequently

$$ME\left(\frac{m}{n} - \frac{M-m}{N-n}\right) = 0 .$$

As shown by Finney (1948) and Latcsha (1953) (see also Fleiss 1981 and Bol'shev & Smirnov 1983 for details), the probability function p of the random variable m at fixed M, N, and n, in the case when properties Y and Z are independent, is given by a hypergeometrical distribution. This distribution can be approximated by a normal, Poisson or binomial distribution, depending on the specific range of variation of the parameters M, N, and n. For $N \geq 25$, independently of M and n, the hypergeometrical distribution of p can be well approximated by an incomplete beta function

$$p \approx I_x(a, b)$$

which is defined in the range $0 \leq x \leq 1$, with $a > 0$ and $b > 0$, by the formula (see Press et al. 1990)

$$I_x(a, b) \equiv \frac{B_x(a, b)}{B(a, b)} \equiv \frac{1}{B(a, b)} \int_0^x t^{a-1}(1-t)^{b-1}\, dt$$

with the limiting values

$$I_0(a, b) = 0 \qquad I_1(a, b) = 1$$

and the symmetry relation

$$I_x(a, b) = 1 - I_{1-x}(b, a) .$$

Here $B(a, b)$ is the beta function

$$B(a, b) = \int_0^1 t^{a-1}(1-t)^{b-1}\, dt .$$

In the case when $2n \geq N$ and $m/n \geq (M-m)/(N-n)$ (conditions which can be made to hold by permuting the rows and columns of the 2×2 contingency table) the parameters x, a, b can be obtained as follows (see Bol'shev & Smirnov 1983)

$$x = \frac{N(n + M - 1) - 2nM}{N(N-2)} \qquad a = m - c \qquad b = n' - m + c + 1 ,$$

where

$$n' = \frac{(N-2)^2}{N-1} \frac{nM(N-n)(N-M)}{[(N-M)(N-n) + nM - N][N(n+M-1) - 2nM]} \qquad c = \frac{nM(M-1)(n-1)}{(N-1)[(N-M)(N-n) + nM - N]} .$$

We are interested here in the case where the total sample is subdivided into two subgroups according, for example, to the property Z of being a bright galaxy or not (i.e., being a BCG). The Y property can be, for example, that of having a nearby (e.g., $D_{NN} \leq 1.8\ h^{-1}$ Mpc) or distant bright neighbor (e.g., $D_{NN} > 1.8\ h^{-1}$ Mpc). The problem is to decide from the subdivision into two subgroups whether the two properties are independent or not.

As an example, we have constructed the 2×2 contingency Table A2 for the volume-limited subsample 9 in Table 4. In Table A2, n is the total number of BCGs, m the number of BCGs having a bright companion with $D_{NN} \leq 1.8\ h^{-1}$ Mpc, $n - m$ the number of BCGs having no bright companion within $1.8\ h^{-1}$ Mpc, $M - m$ the number of bright galaxies with a bright companion within 1.8 h^{-1} Mpc and $N - M - (n - m)$ the number of bright galaxies with no bright companion within $1.8\ h^{-1}$ Mpc.

Adopting the null hypothesis that the properties Y and Z are independent, then the distribution of m for constant M, N, and n is described by a hypergeometrical function. We calculate p according to the above formulae to test the independence of Y and Z for Table A2.

TABLE A1

General Format of a 2 × 2 Contingency Table

Property	Y	Without Y	Sum
Z	m	$n - m$	n
Without Z	$M - m$	$N - n - (M - m)$	$N - n$
Sum	M	$N - M$	N

TABLE A2

An Example of a 2 × 2 Contingency Table

Property	Y ($D_{NN} \leq 1.8\ h^{-1}$ Mpc)	Without Y ($D_{NN} > 1.8\ h^{-1}$ Mpc)	Sum
BCG	4	39	43
CfA	13	26	39
Sum	17	65	82

© American Astronomical Society • Provided by the NASA Astrophysics Data System

1995ApJ...443..499P

We found that for Table A2 if there were no correlation between the properties of being a BCG and that of having a bright companion within $D_{NN} = 1.8\ h^{-1}$ Mpc, the probability to get accidentally the table with the same occupation numbers is less than $p = 0.01$, i.e., the null hypothesis that Y and Z are independent can be rejected at a confidence level $P = 1 - p = 0.99$.

REFERENCES

Ashman, K. M. 1992, PASP, 104, 1109
Baesi-Pillastrini, G. C., Palumbo, G. G. C., & Vettolani G. 1984, A&AS, 56, 363
Bardeen, J. M., Bond, J. R., Kaiser, N., & Szalay, A. S. 1986, ApJ, 304, 15
Barnes, J. E. 1992, in Physics of Nearby Galaxies: Nature or Nurture?, ed. T. X. Thuan, C. Balkowski, & J. T. T. Van (Gif-sur-Yvette: Editions Frontières), 301
Binggeli, B., Tarenghi, M., & Sandage, A. 1990, A&A, 228, 42
Bol'shev, L. N., & Smirnov, N. V. 1983, Tables of Mathematical Tables (Moscow: Nauka Publishers)
Bothun, G. D., Beers, T., Mould, J., & Huchra, J. 1986, ApJ, 308, 510
Bottinelli, L., et al. 1993, A&AS, 102, 57
da Costa, L. N., et al. 1988, ApJ, 327, 544
Davies, J. I., & Phillips, S. 1989, Ap&SS, 157, 291
Davis, M., Efstathiou, G., Frenk, C. S., & White, S. D. M. 1985, ApJ, 292, 371
Dekel, A., & Rees, M. 1987, Nature, 326, 455
Dekel, A., & Silk, J. 1986, ApJ, 303, 39
de Lapparent, V., Geller, M., & Huchra, J. 1986, ApJ, 302, L1
Eder, J. A., Schombert, J. M., Dekel, A., & Oemler, A. 1989, ApJ, 340, 29
Evrard, A. E. 1989, ApJ, 341, 26
Evrard, A. E., Silk, J., & Szalay, A. S. 1990, ApJ, 365, 13
Fairall, A. P., Palumbo, G. G. C., Vettolani, G., Kauffmann, G., Jones, A., & Baiesi-Pillastrini, G. 1990, MNRAS, 247, L21
Fairall, A. P. 1992, private communication
Fanelli, M. N., O'Connell, R. W., & Thuan, T. X. 1988, ApJ, 336, 665
Finney, D. J. 1948, Biometrika, 35, 145
Fleiss, J. 1981, Statistical Methods for Rates and Proportions (New York: Wiley)
Geller, M. J., & Huchra, J. P. 1983, ApJS, 52, 61
Gott, J. R., et al. 1989, ApJ, 340, 625
Henning, P. A. 1992, ApJS, 78, 365
Henning, P. A., & Kerr, F. J. 1989, ApJ, 347, L1
Hopp, U. 1994, in ESO/OHP Workshop on Dwarf Galaxies, ed. G. Meylan & P. Prugniel (Garching: ESO), 37
Huchra, J. P., & Sargent, W. L. W. 1973, ApJ, 186, 433
Huchra, J. P., Davis, M., Latham, D., & Tonry, J. 1983, ApJS, 52, 89
Iovino, A., Melnick, J., & Shaver, P. 1988, ApJ, 330, L17
Izotov, Yu. I., Lipovetsky, V. A., Guseva, N. G., Kniazev, A. Yu., Stepanian, J. A. 1990, Nature, 343, 238
Izotov, Yu. I., Lipovetsky, V. A., Guseva, N. G., Stepanian, J. A., Erastova, L. K., & Kniazev, A. Yu. 1992, in The Feedback of Chemical Evolution on the Stellar Content of Galaxies, ed. D. Alloin & G. Stasinska (Paris: Obs. Meudon), 127
Izotov, Yu. I., Thuan, T. X., & Lipovetsky, V. A. 1994, ApJ, 435, 647
Kaufmann, G., & Fairall, A. P. 1991, MNRAS, 248, 313
Klypin, A., Holtzman, J., Primack, J., & Regos, E. 1993, ApJ, 416, 1
Kraan-Korteweg, R. C. 1986, A&AS, 66, 255
Lacey, C., & Silk J. 1991, ApJ, 381, 14
Latcsha, R. 1953, Biometrika, 40, 74
Markarian, B. E., Lipovetsky, V. A., & Stepanian, J. A. 1983, Astrofizika, 19, 29
Markarian, B. E., Lipovetsky, V. A., Stepanian, J. A., Erastova, L. K., & Shapovalova, A. I. 1989, Comm. Astrophys. Obs., 62, 5
Mirabel, I. F., Dottori, H., & Lutz, D. 1992, A&A, 256, L19
Mirabel, I. F., Lutz, D., & Maza J. 1991, A&A, 243, 367
Moody, J. W., Kirschner, R. P., MacAlpine, G. M., & Gregory, S. A. 1987, ApJ, 314, L33
Ostriker, J. P. 1993, ARA&A, 31, 689
Park, C., & Gott, J. R. 1991, ApJ, 378, 457
Pesch, P., & Sanduleak, N. 1987, ApJS, 63, 809
Press, W. H., Flannery, B. P., Teukolsky, S. A., & Vetterling, W. T. 1990, Numerical Recipes in C (Cambridge: Cambridge Univ. Press), 178
Pustil'nik, S. A., Ugryumov, A. V., & Lipovetsky, V. A. 1993, SISSA preprint no. 86/93/A
Pustil'nik, S. A., Ugryumov, A. V., Lipovetsky, V. A., Thuan, T. X., & Salzer, J. J. 1994, in ESO/OHP Workshop on Dwarf Galaxies, ed. G. Meylan & P. Prugniel (Garshing: ESO), 133
Ramella, M., Geller, M. J., & Huchra, J. P. 1992, ApJ, 384, 396
Rees, M. J. 1988, Highlights Astron., 8, 45
Richter, O.-G., & Huchtmeier, W. K. 1991, A&AS, 87, 425
Salzer, J. J. 1989, ApJ, 347, 152
Salzer, J. J., Hanson, M. M., & Gavazzi, G. 1990, ApJ, 353, 39
Salzer, J. J., & Rosenberg, J. L. 1994, in ESO/OHP Workshop on Dwarf Galaxies, ed. G. Meylan & P. Prugniel (Garshing: ESO), 129
Schmidt, M. 1968, ApJ, 151, 393
Schneider, S. E., Thuan, T. X., Mangum, J. G., & Miller, J. 1992, ApJS, 81, 5
Schneider, S. E., Thuan, T. X., Margri, C., & Wadiak, E. J. 1990, ApJS, 72, 245
Stepanian, J. A., Lipovetsky, V. A., Erastova, L. K., Gyulzadian, M. B., Izotov Yu. I., & Guseva, N. G. 1993c, Astrofiz. Issled., 35, 32
Stepanian, J. A., Lipovetsky, V. A., Erastova, L. K., Hakopian, S. A., Izotov, Yu. I., & Guseva N. G. 1993d, Astrofiz. Issled., 35, 38
Stepanian, J. A., Lipovetsky, V. A., Erastova, L. K., & Shapovalova, A. I. 1987, in IAU Symp. 128, Observational Evidence of Activity of Galaxies, ed. E. Yc. Khachikian, K. J. Fricke, & J. Melnick (Dordrecht: Kluwer), 17
Stepanian, J. A., Lipovetsky, V. A., Erastova, L. K., Shapovalova, A. I., & Gyulzadian, M. B. 1993a, Astrofiz. Issled., 35, 15
Stepanian, J. A., Lipovetsky, V. A., Erastova, L. K., Shapovalova, A. I., & Hakopian, S. A. 1993b, Astrofiz. Issled., 35, 24
Tago, E. 1987, Publications of Tartu Observatory, 52, 163
Thuan, T. X. 1985, ApJ, 299, 881
Thuan, T. X., Alimi, J.-M., Gott, J. R., & Schneider, S. E. 1991, ApJ, 370, 25
Thuan, T. X., Gott, J. R., & Schneider, S. E. 1987, ApJ, 315, L93
Thuan, T. X., Izotov, Yu. I., & Lipovetsky, V. A. 1995a, ApJ, in press
Thuan, T. X., & Martin, G. E. 1981, ApJ, 247, 823
Thuan, T. X., Martin, J.-M., Lipovetsky, V. A., & Pustil'nik, S. A. 1995b, in preparation
Tifft, W. G., Kirschner, R. P., Greogory, S. A., & Moody, J. W. 1986, ApJ, 310, 75
Trimble, V. 1987, ARA&A, 25, 425
Weinberg, D. H., Szomoru, A., Guhathakurta, P., & van Gorkom, J. H. 1991, ApJ, 372, L13
Weistrop, D. 1989, AJ, 97, 357
———. 1994, in Violent Star Formation from 30 Doradus to QSOs, ed. G. Tenorio-Tagle (Cambridge: Cambridge Univ. Press), 100
Weistrop, D., & Downs, R. A. 1988, ApJ, 331, 172
Weistrop, D., Hintzen, P., Kennicutt, R. C., Liu, C., Lowenthal, J., Cheng, K.-P., Oliversen, R., & Woodgate, B. 1992, ApJ, 396, L23

© American Astronomical Society • Provided by the NASA Astrophysics Data System